Volume 57(4): 383–396, 2009
Journal of Histochemistry & Cytochemistry
http://www.jhc.org

ARTICLE

Expression of *Muc19/Smgc* Gene Products During Murine Sublingual Gland Development: Cytodifferentiation and Maturation of Salivary Mucous Cells

Biswadip Das, Melanie N. Cash, Arthur R. Hand, Armin Shivazad, and David J. Culp

Department of Oral Biology, College of Dentistry, University of Florida, Gainesville, Florida (BD,MNC,AS,DJC), and Departments of Craniofacial Sciences and Cell Biology, School of Dental Medicine, University of Connecticut Health Center, Farmington, Connecticut (ARH)

SUMMARY *Muc19/Smgc* expresses two splice variants, *Smgc* (submandibular gland protein C) and *Muc19* (mucin 19), the latter a major exocrine product of differentiated murine sublingual mucous cells. Transcripts for *Smgc* were detected recently in neonatal sublingual glands, suggesting that SMGC proteins are expressed during initial salivary mucous cell cytodifferentiation. We therefore compared developmental expression of transcripts and translation products of *Smgc* and *Muc19* in sublingual glands. We find abundant expression of SMGC within the initial terminal bulbs, with a subsequent decrease as Muc19 expression increases. During postnatal gland expansion, SMGC is found in presumptive newly formed acinar cells and then persists in putative acinar stem cells. Mucin levels increase 7-fold during the first 3 weeks of life, with little change in transcript levels, whereas between postnatal days 21 and 28, there is a 3-fold increase in *Muc19* mRNA and heteronuclear RNA. Our collective results demonstrate the direct transition from SMGC to Muc19 expression during early mucous cell cytodifferentiation and further indicate developmentally regulated changes in *Muc19/Smgc* transcription, alternative splicing, and translation. These changes in *Muc19/Smgc* gene expression delineate multiple stages of salivary mucous cell cytodifferentiation and subsequent maturation during embryonic gland development through the first 4 weeks of postnatal life. **(J Histochem Cytochem 57:383–396, 2009)**

KEY WORDS
mucin
exocrine
alternative splicing
salivary glands

THE GENE *Muc19/Smgc* expresses at least two translation products in mice, SMGC (submandibular gland protein C) and the high-molecular-weight and gel-forming mucin, Muc19 (Culp et al. 2004; Zinzen et al. 2004). Large, gel-forming mucins are abundant organic constituents of saliva and protect the oral cavity through lubrication, hydration, and the selective clearance or adherence of microorganisms (Tabak 1995). In mice, Muc19 is the major secretion product of the mucous acinar cell phenotype of adult sublingual glands (Culp et al. 2004). Interestingly, this cell type and Muc19 expression are essentially absent in the other two major glands of adult mice, the submandibular and parotid glands. In contrast, SMGC was first identified in rat submandibular glands during early postnatal development as an exocrine product of unknown function (Ball and Redman 1984). SMGC is localized to the electron-dense secretion granules of type I cells in developing submandibular glands and is considered a specific marker for this cell type in early cytodifferentiation (Ball et al. 1988a,b). Analogous cells in mice are termed terminal tubule cells (see review by Denny et al. 1997). Another cell type identified in developing submandibular glands, type III cells (rats) or proacinar cells (mice), give rise to mature acinar cells, whereas SMGC-expressing type I or terminal tubule cells gradually diminish in number (Denny et al. 1997; Zinzen et al. 2004). It is currently unclear whether terminal tubule cells and proacinar cells represent two distinct cellular lineages, or whether they are separate transitional stages in the differentiation of submandibular acinar cells (Denny et al. 1997).

Correspondence to: Dr David J. Culp, Department of Oral Biology, University of Florida College of Dentistry, 1600 SW Archer Rd., PO Box 100424, Gainesville, FL 32610-3003. E-mail: dculp@ dental.ufl.edu
Received for publication September 18, 2008; accepted December 5, 2008 [DOI: 10.1369/jhc.2008.952853].

 0022-1554/08/$3.30

Muc19/Smgc is composed of 60 exons and spans at least 105 kb of genomic sequence. *Smgc* is encoded by exons 1–18, whereas *Muc19* transcripts incorporate exon 1 and then skip to exons 19–60 (Culp et al. 2004; Zinzen et al. 2004). Thus, only exon 1 is shared between the two transcripts and encodes for most of the predicted signal peptide directing both translation products to the exocrine secretory pathway. Because these two transcripts each incorporate exon 1, a single heteronuclear RNA can only be spliced to produce one of the two gene products, *Muc19* or *Smgc*. Previously, we detected full-length *Smgc* transcripts in sublingual glands of 3-day-old mice and further discovered the expression in both neonatal and adult glands of a truncated splice variant, *t-Smgc*, encoded by exons 1, 17, and 18 (Culp et al. 2004). The expression of multiple *Muc19/Smgc* gene products in murine sublingual glands indicates that this gene undergoes a complex pattern of regulated expression in these glands.

Given the expression of SMGC in the early development of submandibular glands and our recent findings that *Smgc* transcripts are present in sublingual glands of 3-day-old mice (Culp et al. 2004), we hypothesized that SMGC is expressed during initial cytodifferentiation of sublingual mucous cells. To test this hypothesis, we compared the temporal expression of transcripts and translation products of *Smgc* and *Muc19* in sublingual glands during prenatal and postnatal development. Because SMGC expression is prolonged into adulthood in female submandibular glands (Zinzen et al. 2004), we also compared gender-specific expression of *Smgc* and *Muc19* transcripts. We further assessed relative expression levels of *Muc19* and truncated *Smgc* (*t-Smgc*) in adult sublingual glands, and explored whether *t-Smgc* transcripts are translated. Results are discussed with respect to a putative role for SMGC in the initial cytodifferentiation of sublingual mucous cells. Moreover, upon evaluation of the collective results, we find evidence for temporal changes in *Muc19/Smgc* transcription, alternative splicing, and translation that delineate different stages of salivary mucous cell cytodifferentiation and subsequent maturation.

Materials and Methods

Animals and Collection of Glands

The University of Florida Institutional Animal Care and Use Committee approved all animal procedures. We established a breeding colony of NFS/NCr mice originally obtained from the National Cancer Institute animal program (Charles River Laboratories; Frederick, MD). Animals were anesthetized by CO_2 inhalation and killed by exsanguination (sectioning the aorta). Sublingual glands were excised free of the hilum region. All excised tissues were blotted on filter paper, flash frozen in liquid nitrogen, and stored at −80C. Frozen tissues were quickly weighed prior to use (Mettler MT-5 microbalance; Mettler Toledo, Columbus, OH). For timed pregnancy experiments, each female was paired with a male overnight then caged individually. Embryos were harvested between 5:00 AM and 7:00 AM.

Preparation of cDNA

Frozen tissues were homogenized directly in TRIzol Reagent (Invitrogen; Carlsbad, CA) using a Mini Bead Beater 8 (BioSpec Products; Bartlesville, OK) for 90 sec in the presence of ∼500 mg of silicone carbide beads (1 mm in size). Total RNA was isolated using standard protocols and treated with DNase I using Ambion's DNA-free Reagent Kit (Applied Biosystems; Foster City, CA). Removal of genomic DNA from a given DNase I–treated RNA sample (1 μg) was verified by the inability of the sample to amplify the specific 253-bp mouse microsatellite marker, D1Mit46 (UniSTS 116254), using forward primer 5′-AGTCAGTCAGGGCTACATGATG-3′ and reverse primer 5′-CACGGGTGCTCTATTTGGAA-3′. RNA purity was assessed by capillary electrophoresis (Agilent 2100 Bioanalyzer; Agilent Technologies, Inc., Santa Clara, CA). RNA integrity numbers ranged from 8.8 to 9.6. Poly(A)$^+$ and poly(A)$^-$ RNA fractions were prepared using oligo-dT Mag-beads (Ambion, Inc.; Austin, TX) according to the manufacturer's instructions. Poly(A)$^+$ RNA was double selected, and the two poly(A)$^-$ RNA fractions were pooled. RNA (5 μg) was reverse transcribed with random primers using the High Capacity cDNA Archive Kit (Applied Biosystems), and the resultant cDNA was purified with the QIAquick PCR purification system (Qiagen; Valencia, CA). RNA and cDNA were quantified using the Quant-iT RNA assay kit or the Quant-iT dsDNA HS assay kit with the Qubit fluorometer (Invitrogen).

Real-time PCR

Real-time PCR assays were conducted in triplicate in 20-μl volumes (0.5–40 ng cDNA) using TaqMan gene expression assays (Applied Biosystems) with 6-carboxyfluorescein as reporter dye and ROX as internal passive reference dye, and were performed on an ABI 7900 Sequence Detection System as per the manufacturer's instructions. Specific assays were: (1) Muc19 mRNA, assay Mm01306462_m1 (exons 34–35, context sequence, 5′-ACCAGTATGCCAGCTTCCACCTCGG-3′, amplicon length, 82 bp); (2) Smgc mRNA, assay Mm01306462_m1 (exons 15–16; context sequence, 5′-GCCAGTGTCTCAGGAATGTCAAGTG-3′, amplicon length, 72 bp); (3) 18S RNA, assay Hs99999901_s1 (exon 1; context sequence, 5′-TGGAGGGCAAGTCTGGTGCCAGCAG-3′, amplicon length, 187 bp); and Muc19 heteronuclear RNA, custom assay MUC19HNRNA-MU19 (intron 19 – exon 20; context sequence, 5′-TCAACACAAGAGAGAAATAA-3′,

amplicon length, 93 bp). Products displayed correct amplicon sizes in agarose gels. Raw C_t values were determined with SDS 2.2.1 software (Applied Biosystems). Copy numbers were calculated from standard curves using appropriate DNA templates. Amplification efficiencies ranged from 0.90 to 1.01 (Rasmussen 2001). Each assay was conducted on three to eight glandular cDNA samples prepared independently from mice in each age group. Results (copy number/ng cDNA) were normalized to 18S RNA (copy number/ng cDNA). Statistical comparisons were conducted using the unpaired, two-tailed *t*-test with Prism 4.0 software (Graphpad Software Inc.; San Diego, CA).

PCR Conditions

Standard conditions for PCR reactions (10–50 ng cDNA) were: 3 min at 98C, 23–40 cycles of 45 sec at 94C, 30 sec at 60C, and 30 sec at 72C followed by 7 min at 72C. Products were resolved in 1.5% agarose gels made in TAE buffer with 0.1% ethidium bromide. Primers were from Invitrogen and included: *t-Smgc* (forward, 5′-ACAGTCTCTACACTTCGGTCCCA-3′ and reverse, 5′-GGATGACCAGTCACAAA CACATC-3′, Zinzen et al. 2004); *Muc19* (forward, 5′-GATTATGCGATTGGTTCATCCT-3′ and reverse, 5′-GTGCAATGTCCCTGAACTCATA-3′, Chen et al. 2004); *Muc2* (forward, 5′-TGTGGCCTGTGTGGGAACTTT-3′ and reverse, 5′-CATAGAGGGCCTGTCCTCAGG-3′, Escande et al. 2004); *Muc5ac* (forward, 5′-GAGGGCCCAGTGAGCATCTCC3′ and reverse, 5′-TGGGACAGCAGCAGTATTCAGT-3′, Escande et al. 2004); *Muc5b* (forward, 5′-TCCTGCTCTGGAATATCCAAG-3′ and reverse, 5′-GCCTCGGGGAGCTTGCCTGCC-3′, Escande et al. 2002); *Muc6* (forward, 5′-TGTGGCTTGTGTGGCAACGCC-3′ and reverse, 5′-TGGTCGAAGTACTCATTCTGG-3′, Escande et al. 2004); *Muc16* (forward, 5′-GCACCACCAAATACCAGCAAAC-3′ and reverse, 5′-GATGAGAATGATAGCCCAGAAAGG-3′); *β-actin* (forward, 5′-CACCTTCCAGCAGATGTG-3′ and reverse, 5′-AAATCCTGAGTCAAAAGCG-3′); and 18S rRNA (forward, 5′-ACGGCTACCACATCCAAGGAAG-3′ and reverse, 5′-GGACACTCAGCTAAGAGCATCGAG-3′). All reactions were run in Qiagen's Taq PCR Master Mix, except for *t-Smgc*, which incorporated the FailSafe PCR buffer system (Epicentre; Madison, WI) as described by Zinzen et al. (2004). PCR products were confirmed by direct sequencing of gel-purified bands (QIAquick Gel Extraction Kit; Qiagen). Sequencing was performed at the University of Florida Interdisciplinary Center for Biotechnology Research using an Applied Biosystems 3100 Genetic Analyzer ABI and Big Dye version 3.1 chemistry.

For semi-quantative PCR of *Muc19* and *t-Smgc* transcripts, random primed cDNA from sublingual glands of 8-week-old mice was diluted to 0.05 ng/μl and 0.02 pg/μl stocks and used in two separate sets of PCR reactions with increasing amounts of cDNA. Digital images of gels were obtained with a Scion Grayscale 1394 Digital Camera (Fotodyne; Hartland, WI). Mean pixel intensities of each individual signal of *t-Smgc* and *Muc19* were determined using Kodak Molecular Imaging Software, v4.0 (Eastman Kodak Co.; Rochester, NY). Background pixel intensities were estimated from an empty lane and used to calculate net mean pixel intensities. Resultant net pixel intensities were plotted as a function of input cDNA, and linear regressions were determined using Prism 4.0 software (Graphpad Software, Inc.).

Fractionation of Glands Into Nuclei and Nuclei-free Fractions

Sublingual glands were excised from ten 8-week-old mice and chilled immediately in ice-cold PBS supplemented with 0.5 mM PMSF. Glands were transferred to homogenizing medium (0.1 M sucrose, 5 mM $CaCl_2$, 3 mM $MgCl_2$, 0.1 mM EDTA, 1 mM dithiothreitol (DTT), 10 mM Tris-HCl, pH 8.0, 0.1 mM PMSF, and 3 U/ml RNase inhibitor), minced, and homogenized in a Dounce homogenizer (10 strokes with a loose-fitting pestle B and 35 strokes with a tight-fitting pestle A) followed by 25 strokes in a glass-teflon homogenizer. The homogenate was then centrifuged at 500 × g for 1 min at 4C. The pellet was homogenized again with a glass-teflon homogenizer for 5 strokes, pooled with the original supernatant, and filtered through 30-μm nylon mesh, and the filtrate was centrifuged at 1200 × g for 8 min at 4C. The supernatant was centrifuged as before. Pellets from each spin were resuspended in 1 ml buffered sucrose (0.25 M sucrose, 5 mM $CaCl_2$, 3 mM $MgCl_2$, 0.1 mM EDTA, 1 mM DTT, 10 mM Tris-HCl, pH 8.0, 0.1 mM PMSF, and 3 U/ml RNase inhibitor), combined, diluted to 5 ml with sucrose buffer, and centrifuged at 1200 × g for 8 min to wash the nuclei. Washing was repeated twice, and the final pellet of nuclei was resuspended in 0.5 ml storage buffer (40% glycerol, 5 mM $CaCl_2$, 3 mM $MgCl_2$, 1 mM EDTA, 1 mM DTT, 10 mM Tris-HCl, pH 8.0, 0.1 mM PMSF, and 6 U/ml RNase inhibitor). The yield of nuclei per preparation ranged from 5×10^7 to 10^8, as determined by counting with a hemocytometer. Total RNA was isolated from equivalent proportions of the nuclei and the nuclei-free fractions (supernatant from the second centrifugation), and cDNA was prepared as described above. cDNA samples (50 ng) from three independent preparations were used in subsequent PCR reactions to amplify *t-Smgc* as described above. Nuclear contamination of nuclei-free fractions was determined from the ratio of *Muc19* heteronuclear transcripts detected in nuclei versus nuclei-free fractions, as assessed by real-time PCR as described above. Ratios of at least 250 were obtained.

Immunohistochemistry

Whole or minced tissues were fixed for 5 hr in 4% paraformaldehyde in PBS then stored at 4C in 1% paraformaldehyde in PBS. Sections (5 μm) were deparaffinized and treated for 10 min in 5% urea containing 50 mM β-mercaptoethanol at 95C to unmask antigenic sites. Sections were then probed with rabbit anti-mouse SMGC or preimmune serum (1:2500 or 1:5000) (Zinzen et al. 2004), or rabbit antiserum raised against purified rat sublingual mucin (Man et al. 1995) or preimmune serum (1:300), as described previously (Fallon et al. 2003), except that we used a Vectastain ABC-HRP kit with Vector Red substrate (Vector Laboratories; Burlingame, CA) and counterstained with hematoxylin.

SDS-PAGE and Western Blots

Frozen glands were immediately weighed, and 10–20 mg wet weight of tissue was placed in 300 to 500 μl of Invitrogen Sample Buffer (Invitrogen). Samples were then sonicated (4 × 10 sec pulses at 30 sec intervals) with a Branson Digital Sonifier 250 at 30% amplitude (Branson Ultrasonic Corp.; Danbury, CT). The samples were then boiled for 10 min and centrifuged (10,000 × g) for 10 min at 4C. Supernatant aliquots of volumes equivalent to 300 μg wet weight of original tissue were applied directly to 4–12% NuPAGE Bis-Tris gradient gels (Invitrogen). Gels were blotted onto polyvinylidene difluoride (PVDF) membranes (Sequi-Blot PVDF Membrane, 0.2 μm; Bio-Rad Laboratories, Hercules, CA) and probed overnight with rabbit anti-mouse SMGC (1:10,000) (Zinzen et al. 2004). This antiserum was raised against His_6 fusion proteins encoded by exons 3–18 of *Smgc*. Buffers and detection reagents were from the WesternBreeze Chemiluminescent Western Blot Immunodetection Kit (Invitrogen) and BioMax Light film (Eastman Kodak Co.). Each experimental condition was performed at least three times. Gland homogenates assayed for Muc19 glycoproteins by SDS-PAGE were processed in a similar manner, except that 50 μg wet weight of original tissue was loaded in each lane. Three separate sample preparations from each age group were run on two gels simultaneously in the same apparatus. The gels were stained simultaneously with Alcian blue, followed by subsequent silver enhancement of Alcian blue staining as described previously (Fallon et al. 2003). Silver enhancement of Alcian blue precedes any staining of proteins (Jay et al. 1990). Digital images were then obtained, and net mean pixel intensities of each lane were determined as described above.

Materials

Unless indicated, all materials were from Sigma Chemical Co., St. Louis, MO. All kits were used according to the manufacturers' instructions.

Results

Expression of *Smgc* and *Muc19* Transcripts During Embryonic and Postnatal Development

We compared the relative levels of transcripts for *Smgc* and *Muc19* mRNAs during sublingual gland embryonic and postnatal development, starting at embryonic day 15 (E15), when the initial epithelial bud has undergone significant branching morphogenesis (Laj et al. 1971). Transcript levels were normalized to 18S RNA, and results were segregated by sex after birth. We also recorded glandular wet weights as a corresponding measure of total gland mass. As shown in Figure 1A, *Smgc* transcripts are first detectable, but variable, at E17. Transcripts increase 3- to 4-fold to peak levels at E19 and E20 ($p=0.45$, E18 versus E19) but then decline at birth, which is between E20 and E21 for the NFS/NCr mouse strain. *Muc19* transcripts during embryological development are barely detectable at E17 and E18, readily detected at E19, and then increase more than 2-fold at E20 (Figure 1B). Interestingly, gland wet weight does not change appreciably during E17 through E19, but then increases ~50% between E19 and E20 (Figure 1D).

Differences are noted between males and females in the expression of *Smgc* transcripts during postnatal development. Females display a relatively constant level of expression from birth through postnatal day 14 (P14), whereas *Smgc* expression in males is transient, peaking at P10 and then becoming essentially undetectable after P21. These gender differences are statistically significant ($p<0.05$) at P0, P3, and P14. Low levels of *Smgc* transcripts continue to be detected in females up to 160 days of age. *Muc19* transcripts are relatively constant from E20 through P21. At P28, there is an approximate 3-fold increase in *Muc19* transcript levels that persists into adulthood ($p<0.05$ for P21 versus P28 and later for each sex). Unlike *Smgc* transcripts, levels of *Muc19* do not vary between males and females throughout postnatal development ($p>0.39$ in all cases). Given the large increase in *Muc19* expression between P21 and P28, we further measured *Muc19* heteronuclear RNA levels as a marker for the rate of *Muc19* transcription (Johnson et al. 2002). As shown in Figure 1C, the relative abundance of heteronuclear RNA mirrored that of *Muc19* transcripts across the different developmental ages. Gland wet weight during postnatal development is initially stagnant through P3, but then increases ~7-fold by P21, reaching ~70% of adult gland weight (Figure 1D).

Immunohistochemical Localization of SMGC During Gland Development

Given the variability of *Smgc* transcript levels during gland development, we evaluated tissue samples for SMGC at all time points that correspond to our measurements of transcripts, through 8 weeks of age. As

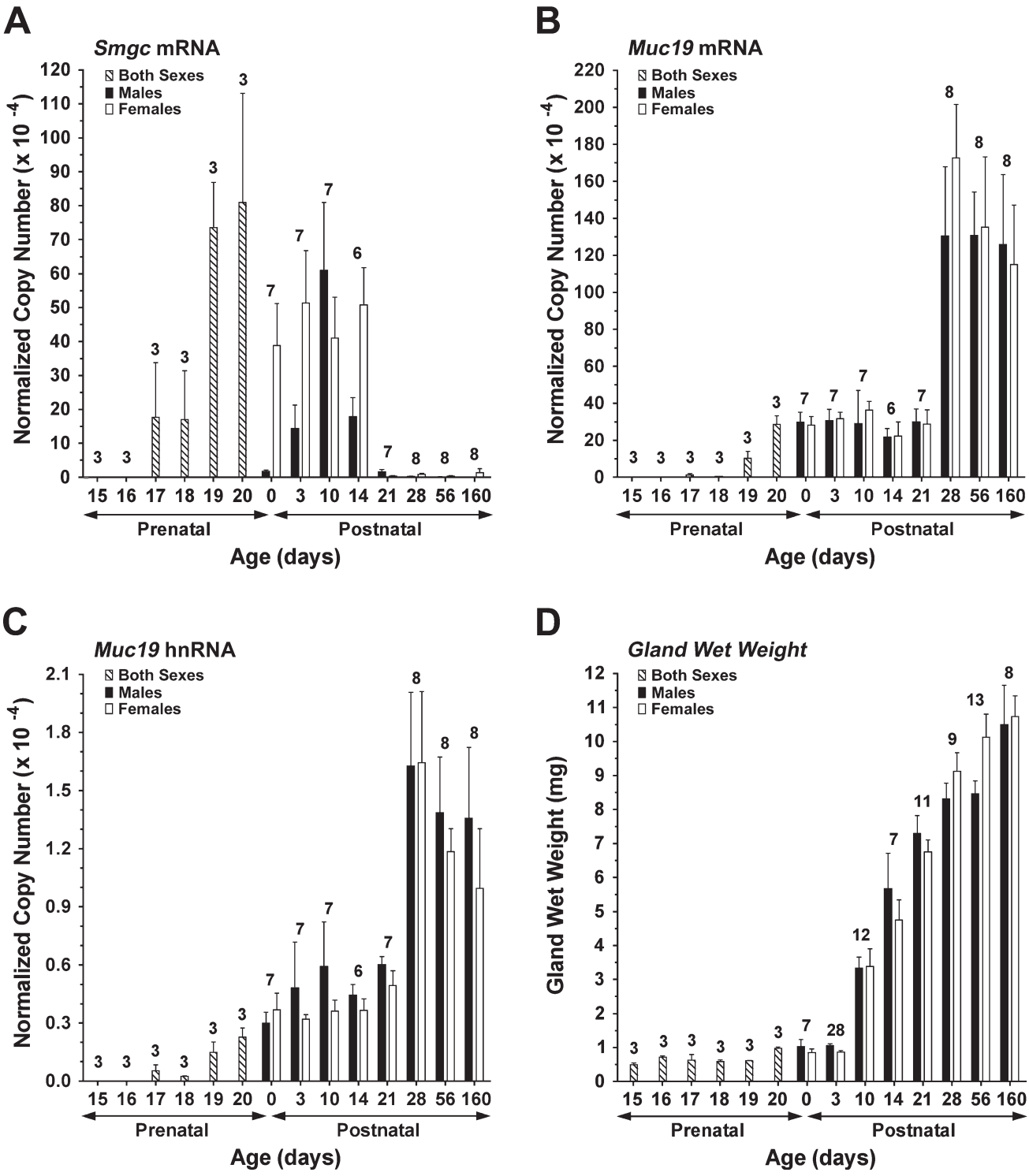

Figure 1 Expression of *Muc19/Smgc* gene products and gland mass during sublingual gland development. cDNA from each preparation of glands was assayed by real-time RT-PCR for submandibular gland protein C (*Smgc*) mRNA (**A**), mucin 19 (*Muc19*) mRNA (**B**), and *Muc19* heteronuclear RNA (**C**). Transcript copy numbers/ng cDNA were normalized to 18S RNA and are shown as means ± SE. 18S RNA levels were consistent from embryonic day 17 (E17) and later (mean ± SE, $13.1 \pm 0.2 \times 10^{10}$ transcripts/ng cDNA). Values were lower at E15 ($3.8 \pm 1.1 \times 10^{10}$ transcripts/ng cDNA) and E16 ($6.0 \pm 0.2 \times 10^{10}$ transcripts/ng cDNA). (**D**) Gland wet weights. Values are means ± SE. Hatched bars, unsexed prenatal glands. Black bars, male glands. Open bars, female glands. Numbers over bars indicate gland preparations per age group (1 to 20 glands/preparation), with equal preparations for each sex. The same preparations were used in panels **A–C**, whereas additional preparations were incorporated for determining gland weights.

shown in Figure 2, all cells within the terminal epithelial bulbs at E17 display strong SMGC staining (Figure 2A). At the distal ends of branching acini are pyramidal-shaped cells with very strong cytoplasmic reactivity and large basal nuclei (Figure 2A, arrowheads). When sectioning produces a thin slice of cytoplasm, these cells clearly contain distinct small and intensely stained granules in the apical cytoplasm, histological characteristics of the serous cell phenotype (not shown). Located in more-proximal regions near the ductal cells (Figure 2A, asterisk) are cells with a basal nucleus and with a large cytoplasm displaying intermediate and diffuse staining (Figure 2A, arrow). Light staining is observed within the lumen of a duct composed of cuboidal cells (Figure 2A, asterisk). At E18, the larger and more-proximal cells of the terminal bulbs are more abundant and display moderate flocculent-like cytoplasmic staining for SMGC (Figure 2B, arrows). Small pyramidal-shaped cells with strong SMGC immunoreactivity are still observed at the distal ends of acini (Figure 2B, arrowhead). SMGC staining at E19 is more variable, with some acini containing cells with intense staining (Figure 2C, arrowheads), whereas many acini are composed of cells with lighter cytoplasmic staining (Figure 2C, arrow).

At E20, just prior to birth, there is a noticeable difference in acinar structures. Most acini are composed of mucous cells with a prominent apical cytoplasm and a compressed basal nucleus. Apparent are acini with clearly formed mucous tubuloacinar structures. Shown in Figure 2D (asterisk) is a branched, V-shaped mucous tubuloacinus. Occasionally seen are fully mature mucous cells in which the apical cytoplasm is even more expanded (Figure 2D, arrow). These characteristics are consistent with prior observations of newborn rodent sublingual glands in which acini are well-developed, displaying the morphological appearance of adult glands (Leeson and Booth 1961; Redman and Ball 1978). SMGC staining at this stage is mainly confined to the cytoplasm of acinar cells and varies from moderate to very light.

At 3 days of age, light SMGC staining is seen in the perinuclear region of mucous acinar cells (Figure 2E). Mucous acini appear larger, on average, and are more compact because the surrounding mesenchymal cells have become mostly depleted. Occasionally, an acinar cell displays very strong granular cytoplasmic staining (Figure 2E, arrowhead). A week later, the cellular architecture and staining pattern is mostly unchanged, except that perinuclear staining is much less prevalent (Figure 2F). Acinar cells with strong cytoplasmic staining are less prevalent in sections, but shown is a rare example of a group of stained acinar cells (Figure 2F, arrowheads). Also shown are two adjoining and unstained intercalated ducts in cross section (Figure 2F, arrow). At 4 weeks of age (Figure 2G), there is little SMGC immunoreactivity, with only light staining in the perinuclear region of the occasional acinar cell (Figure 2G, arrowhead) or within the cytoplasm of a subpopulation of intercalated duct cells (Figure 2G, arrow). No differences were observed in the staining patterns for SMGC between males and females at all postnatal ages assayed (not shown).

An unexpected finding during the immunolocalization studies was the strong cytoplasmic staining for SMGC in a subpopulation of cells lining the lumens of developing large extralobular excretory ducts (Figure 2H). Similar staining of extralobular ducts was observed at all embryonic ages studied as well as at postnatal day 3 (not shown).

Immunohistochemical Localization of Muc19 During Gland Development

To assess Muc19 glycoprotein expression during gland development, we used our antiserum raised against purified rat sublingual mucin (Man et al. 1995). In mouse sublingual glands, this antiserum cross-reacts with high-molecular-weight glycoproteins and is localized specifically to secretion granules of mucous cells (Fallon et al. 2003). Furthermore, antiserum reactivity correlates with attenuated expression of mucous cells and Muc19 glycoproteins in a mutant mouse model (Fallon et al. 2003). To further establish that the antiserum functions as a marker of Muc19 in murine sub-

Figure 2 Immunohistochemical localization of SMGC during sublingual gland development. Ages are indicated in the lower left corner of each panel. (**A**) Staining in early terminal epithelial bulbs. Arrowheads, immunoreactive pyramidal cells at distal ends of branching tubuloacini. Arrow, cells in more-proximal regions, with basal nuclei and larger cytoplasm that display intermediate staining. Asterisk, duct containing a central lumen within branching tubuloacinus. (**B**) A day later, proximal cells of terminal bulbs are more abundant and display moderate flocculent-like cytoplasmic staining (arrows). Arrowhead, strong immunoreactivity by small pyramidal cells at the distal end of a branching tubuloacinus. (**C**) Staining is more variable at E19. Arrowheads, acinar cells with intense staining. Arrow, acinus with lighter cytoplasmic staining. (**D**) Mucous tubuloacini are apparent shortly before birth. Asterisk, a branched V-shaped mucous tubuloacinus with light granular cytoplasmic staining. Arrow, fully mature mucous cell with an unstained and expanded cytoplasm. (**E**) Light staining in the perinuclear region of mucous acinar cells at 3 days of age. Arrowhead, acinar cell with strong granular cytoplasmic staining. (**F**) Mucous acinar cells are mostly unstained. Arrowheads, rare example of a group of strongly stained acinar cells. Arrow, two adjoining intercalated ducts in cross section. (**G**) Most cells are unstained at 4 weeks of age. Arrowhead, light perinuclear staining of an acinar cell. Arrow, subpopulation of intercalated duct cells with light staining. Asterisk, lumen of intercalated duct. (**H**) Strong staining of a subpopulation of cells lining the lumen of a large embryonic extralobular excretory duct. See Results for details. Vector Red substrate with hematoxylin counterstain in all cases. Bar = 35 μm.

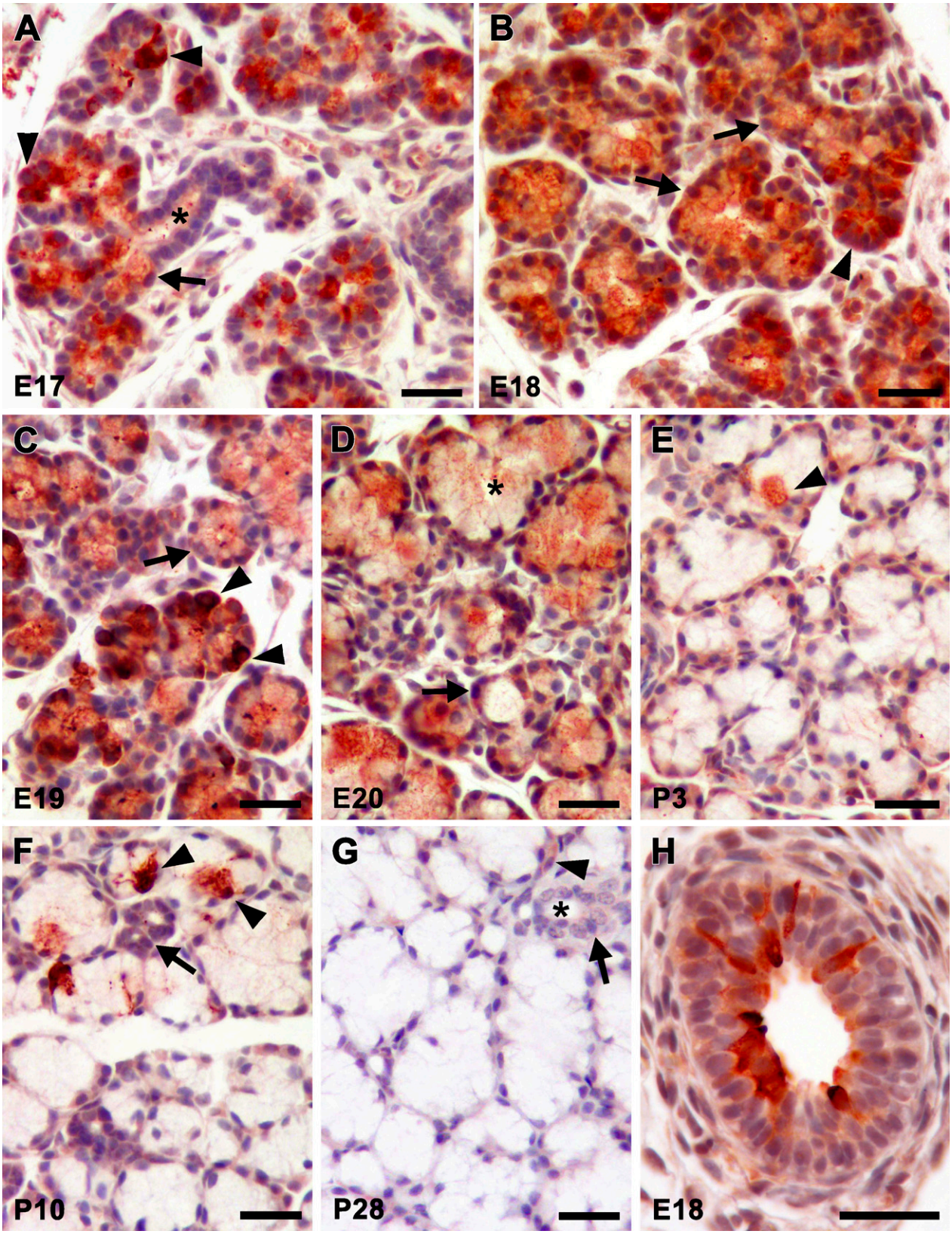

The Journal of Histochemistry & Cytochemistry

lingual glands, we screened glands from 3-day-old and adult mice for expression of transcripts of other secreted high-molecular-weight and gel-forming mucins (i.e., Muc2, Muc5ac, Muc5b, and Muc6) (Thornton et al. 2008) as well as for Muc16, a large membrane-associated mucin localized recently to the cytoplasm of mucous cells of human airway submucosal glands (Davies et al. 2007). As shown in Figure 3, transcripts of other mucins are not detected in murine sublingual glands, indicating that Muc19 is the only large secreted mucin in these glands. In addition, high-molecular-weight glycoprotein expression and antiserum immunoreactivity are absent in sublingual glands of mice with targeted deletion of Muc19 transcripts (Culp, unpublished data).

Histologically, mucous cell cytodifferentiation is well recognized in sublingual glands at birth (Leeson and Booth 1961; Redman and Ball 1978). In addition, we demonstrated previously that glands at 3 days of age are predominantly composed of mucous tubuloacini that are immunoreactive with our anti-mucin antiserum (Fallon et al. 2003), consistent with results above, indicating that *Muc19* transcript levels increase to a plateau at E20 that is maintained through P21. Thus, given that Muc19 expression correlates with the early mucous cell cytodifferentiation in sublingual glands, we assessed mucin immunolocalization in sections during prenatal gland development and in adult animals. Shown in Figure 4A are two long terminal tubules at E17 that form an inverted V-shape, intersecting at the top of the figure. Anti-mucin reactivity is restricted mostly to the apical cytoplasm of the larger proximal cells of terminal bulbs (Figure 4A, arrows). The more proximal ducts are unstained (Figure 4A, asterisk). In contrast to SMGC staining, cells at the distal ends are negative (compare structures indicated by arrowheads in Figure 4A with those in Figure 2A). Anti-mucin staining at E18 is similar to E17, except for the expansion of the larger immunoreactive cells within the proximal regions of terminal bulbs (Figure 4B, arrows). At E19, acini composed of larger columnar cells with strong cytoplasmic staining are more apparent (Figure 4C arrow). Terminal bulbs with negatively stained cells at the distal ends are still observed (Figure 4C, arrowhead).

As noted above, there is a marked morphological transformation of the gland between E19 and E20. Shown in the upper portion of Figure 4D is a large mucous tubuloacinus with a clearly defined lumen that spans between the two asterisks. Cells lining the tubuloacinus are columnar in shape with a basally compressed nucleus and a cytoplasm filled with strong anti-mucin immunoreactivity, features typical of well-developed mucous cells (Figure 4D, arrow). At E20, the lesser-developed terminal bulbs without anti-mucin staining that were observed earlier are rarely delineated in sections (not shown). In Figure 4E, we show a section from an adult gland (P56) that demonstrates the strong immunostaining of mature mucous cells, the abundance of mucous tubuloacini, and an unstained ductal structure.

Glandular SMGC Protein and Muc19 Glycoprotein Expression During Postnatal Development

A Western blot for SMGC in whole-gland homogenates from male and female mice at postnatal days 3 through 56 is shown in Figure 5. SMGC proteins are abundant in 3-day-old glands from male and female mice, although levels are less than in adjoining submandibular glands (control, far left lane). The expression pattern is very similar to that in submandibular glands, with a major band at ~105 kDa, multiple species of lesser mass, and two low-abundance species at higher mass. With increasing age, we find variable levels of expression. SMGC levels in both sexes are lower at 10 days of age, but then increase at 14 days. At 21 days of age, expression levels for each sex are quite variable among different samples. Shown in Figure 5 are examples of the highest- and lowest-expressing samples at this age. More consistent though is a marked decrease in expression at 28 days. When blots are exposed to film for longer times, very low levels of the major 105 kDa species as well as many species of lower mass are detectable in 28-day- and 56-day-old glands (Figure 5). Also apparent in nearly all samples are two bands of ~150 kDa and 200 kDa.

We used direct staining of SDS-PAGE gels with Alcian blue followed by silver enhancement to assess glandular Muc19 expression (Figure 6A). Previously, we demonstrated that Muc19 accounts for high-molecular-weight glycoproteins discernable by this method (Fallon et al. 2003). As shown in Figure 6B, glycoprotein expression

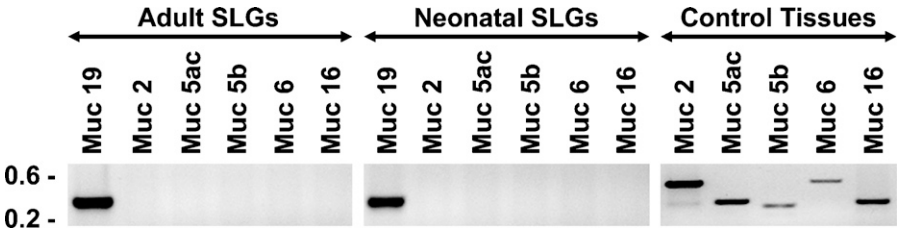

Figure 3 Expression of transcripts for large mucins in adult and neonatal (3-day-old) sublingual glands. RT-PCR was performed using 50 ng of cDNA, 30 cycles, and primers specific for the indicated mucin transcripts (see Materials and Methods for details). Shown are representative results from three independent preparations of cDNA from each age group. Tissues serving as positive controls for transcripts absent in sublingual glands were ileum (*Muc2*), stomach (*Muc5ac* and *Muc6*), tracheolarynx (*Muc5b*), and ovaries (*Muc16*).

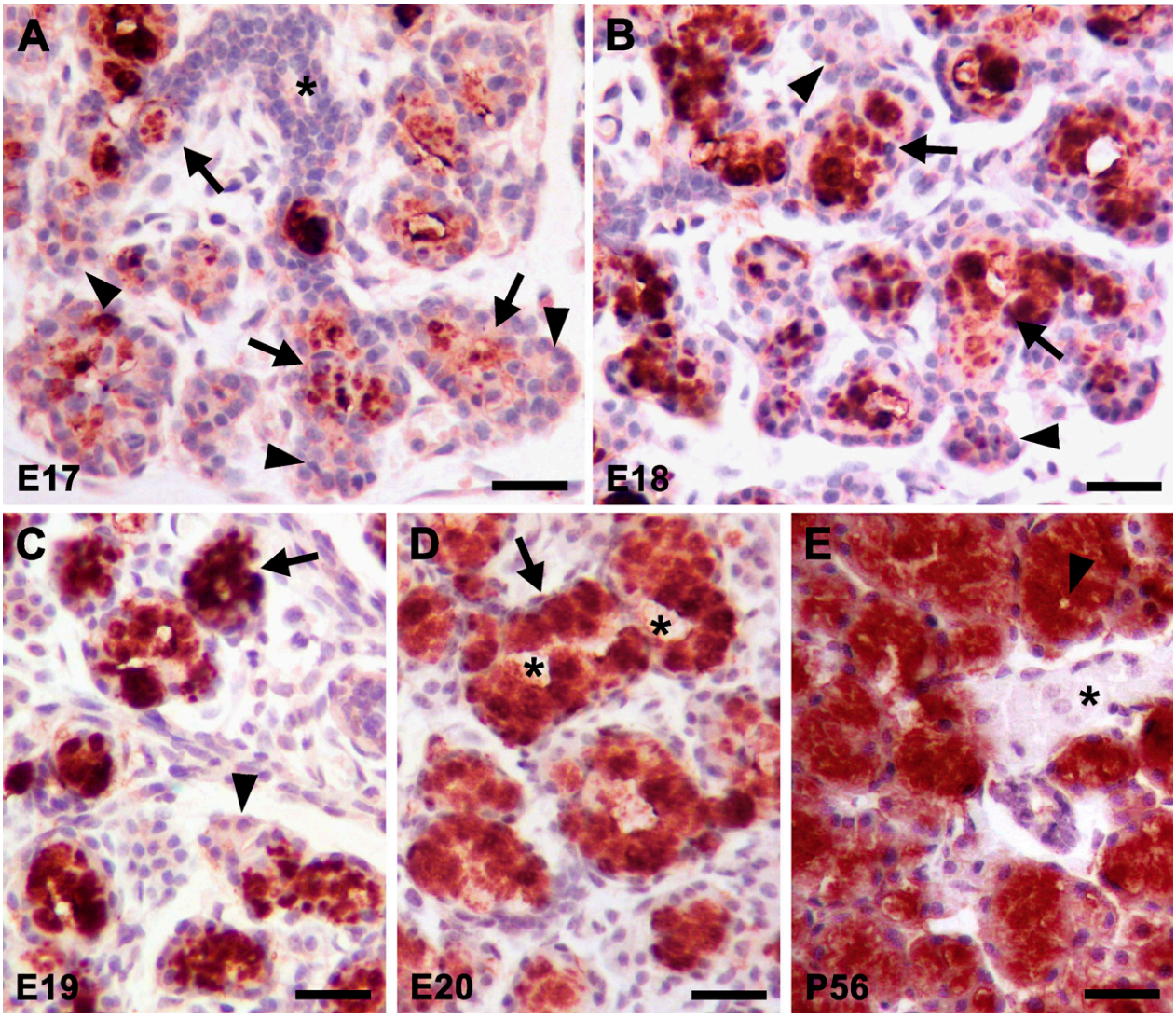

Figure 4 Immunohistochemical localization of Muc19 during sublingual gland development. Ages are indicated in the lower left corner of each panel. (**A**) Staining in early terminal bulbs is localized to the apical cytoplasm of the larger proximal cells (arrows). Arrowheads, absence of staining in pyramidal cells at distal ends of branching tubuloacini. Asterisk, lumen of duct at proximal end of terminal tubule. (**B**) Immunoreactive proximal cells are more abundant at E18 (arrows). Distal ends of terminal bulbs are unstained (arrowheads). (**C**) Acini with strongly stained columnar cells are apparent the following day (arrow). Arrowhead, unstained cells at the distal end of a terminal bulb. (**D**) Mucous tubuloacini are apparent at E20 and display strong immunoreactivity. Two asterisks demark the ends of a lumen within a large mucous tubuloacinus. Arrow, tall columnar mucous acinar cells with basally compressed nuclei and strongly stained cytoplasm. (**E**) Intensely stained mucous tubuloacini of an adult gland. Arrowhead, acinar lumen. Asterisk, unstained ductal structure. See Results for details. Vector Red substrate with hematoxylin counterstain in all cases. Bar = 35 μm.

in glandular homogenates increases markedly during the first 21 days of postnatal development and then begins to level out, with a trend toward a more gradual increase up to 56 days of age.

Relative Expression of and Exploring the Nature of *t-Smgc* in Adult Sublingual Glands

In light of the coexpression of transcripts for *t-Smgc* with *Muc19* in sublingual glands of neonates and adults (Culp et al. 2004), it is of interest to delineate the relative expression levels of these two splice variants of the gene *Muc19/Smgc*, and to explore whether *t-Smgc* results in a translated product. It should first be noted that the real-time PCR assay used to detect *Smgc* incorporates primers to exons 15 and 16, and thus does not detect *t-Smgc*. Instead, this assay detects full-length *Smgc* and most low-abundant splice variants identified previously in submandibular glands (Zinzen et al. 2004). We tested a TaqMan assay that targets

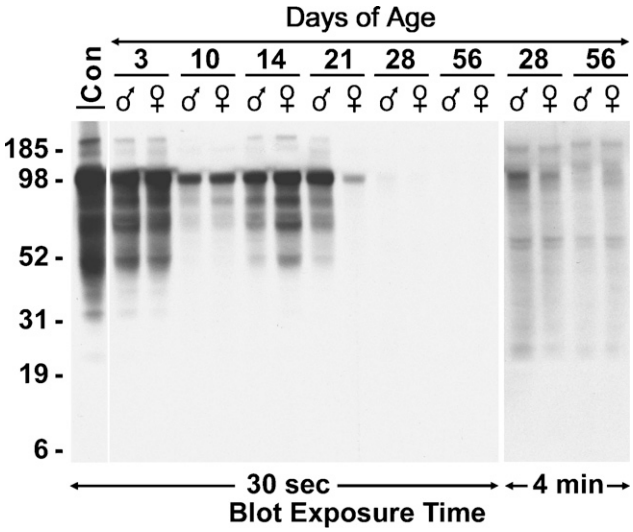

Figure 5 Western blot of SMGC in whole-gland homogenates at postnatal days 3 through 56. Postnatal days of age and sexes are indicated above the lanes. Far left lane is a control (Con) from a 3-day-old submandibular gland. All lanes were loaded with the equivalent of 300 μg wet weight of tissue and run on a 4–12% gradient gel. The blot was initially exposed to film for 30 sec. The lanes corresponding to ages 28 days and 56 days were re-exposed to film for 4 min to distinguish less-abundant proteins. Mobilities of molecular mass markers (kDa) are indicated on the left.

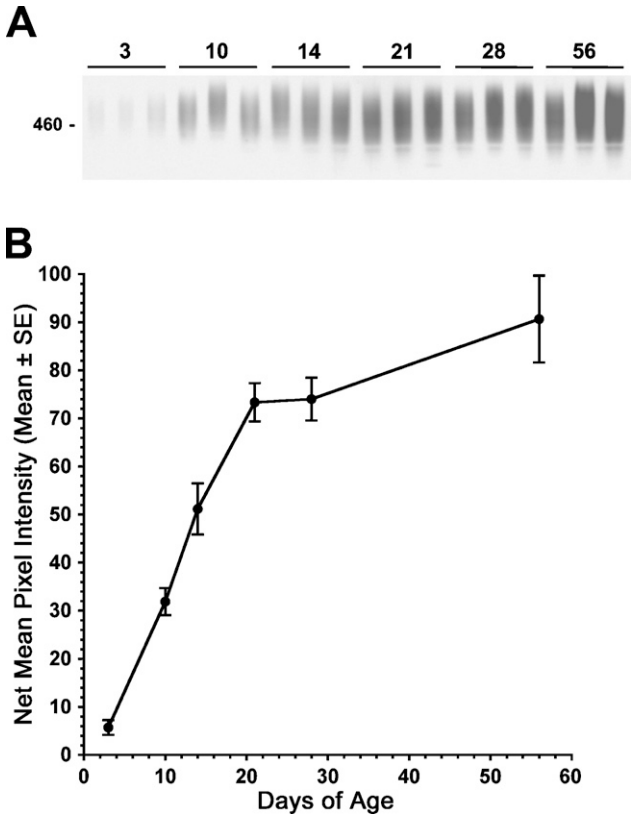

Figure 6 Muc19 in whole-gland homogenates at postnatal days 3 through 56. Three separate sample preparations from each age group were run on 4–12% SDS-PAGE gels (50 μg wet weight of tissue/lane) and stained with Alcian blue followed by silver enhancement. (**A**) Image of the stained glycoproteins in each lane. Ages are given above the lanes. (**B**) Graph of the net mean pixel intensities in the lanes shown in **A**, expressed as mean ± SE for the triplicate values of each age group.

exons 17 and 18 of *Smgc*, but it gave false-positive results. We therefore resorted to a semi-quantitative PCR assay to evaluate *t-Smgc* expression. The results shown in Figure 7A indicate that *t-Smgc* transcripts in 8-week-old sublingual glands are only ~0.04% of *Muc19* transcript levels.

We further addressed whether *t-Smgc* may encode a putative translation product. Predicted translation of *t-Smgc* results in an acidic (pI 4.8) protein of 128 residues, rich in serine and glycine (17.8% each) and with a predicted mass of 12.6 kDa. This predicted protein is essentially a truncated version of SMGC, inasmuch as it incorporates the same codons in exons 1, 17, and 18 as those encoding SMGC, including an initial 20-residue signal peptide predicted by the SignalP program (v3.0; http://www.cbs.dtu.dk/services/SignalP). Cleavage of the signal peptide reduces the protein to 10.5 kDa. Nevertheless, in Western blots (Figure 5), we are unable to detect anti-SMGC-reactive species of less than 25 kDa in sublingual glands in any of the age groups. Similar results are obtained when blots are overexposed (Figure 5 and not shown).

Given the low abundance and small size of *t-Smgc*, we further explored the nature of this small RNA species. In identifying *t-Smgc* transcripts by RT-PCR (above), we used total RNA and primers to exons 1 and 18, an approach that does not distinguish polyadenylated *t-Smgc*. We therefore probed for *t-Smgc* in random, primed cDNAs produced from total, poly(A)$^+$, and poly(A)$^-$ RNA. As shown in Figure 7B, transcripts for *t-Smgc* are only present in total RNA and poly(A)$^+$ RNA. Additionally, we found significant levels of *t-Smgc* transcripts in nuclei-free fractions of gland homogenates, suggesting that polyadenylated *t-Smgc* mRNA is transported out of the nucleus (Figure 7C). Finally, we screened for *t-Smgc* expression in the other two major salivary glands, the parotid and submandibular glands, of adult mice. Transcripts for *t-Smgc*, as well as for Muc19, are not detected in these other two glands, but display a strong signal in sublingual glands (Figure 7D). Two larger transcripts of much lower abundance are also detected in sublingual glands, probably due to larger splice variants of *Smgc*.

Discussion

Analyses of the temporal expression of *Muc19/Smgc* gene products during sublingual gland development argue for expression of SMGC directly preceding that

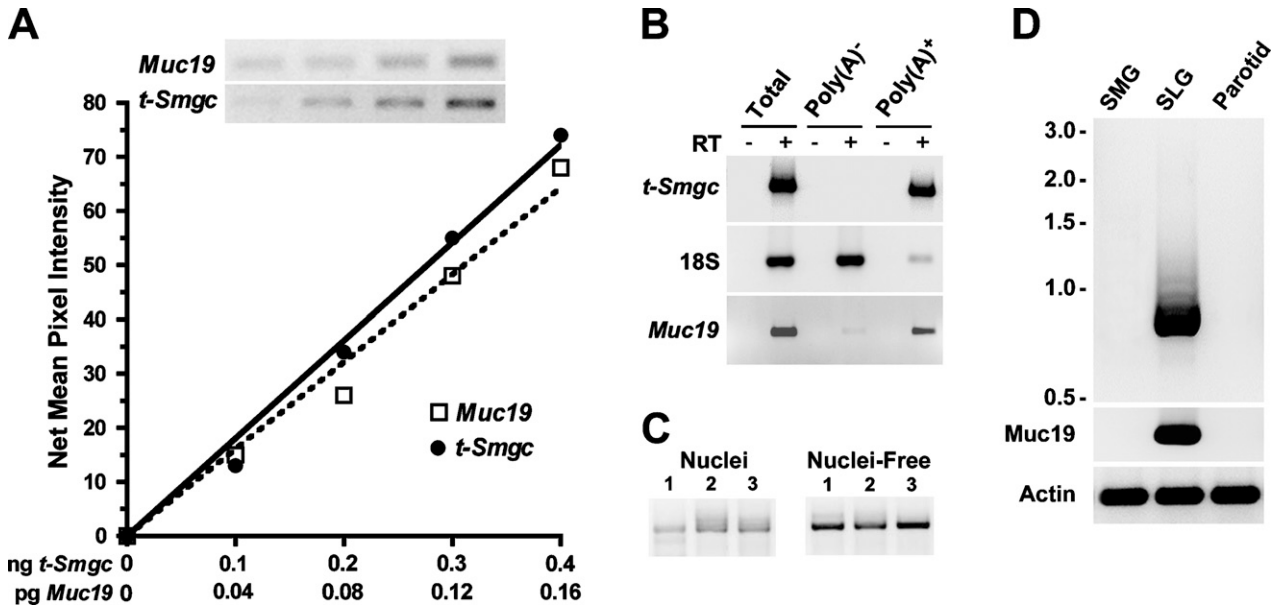

Figure 7 Evaluation of *t-Smgc* transcripts in 8-week-old mice. (**A**) Semi-quantitative comparison of *Muc19* and *t-Smgc* transcripts in sublingual glands. Increasing amounts of random primed cDNA (x-axis) were probed by PCR (35 cycles) with primers to *Smgc* (exons 1 and 18) and the 3′ end of *Muc19*. Products were run on a 1.5% agarose gel (insert). Net mean pixel intensity of each band was determined and plotted versus the amount of input cDNA. Slopes of the lines (net mean pixel intensity/ng cDNA) are from linear regressions ($r^2 > 0.98$) and were 4.0×10^5 (*Muc19*) and 1.8×10^2 (*t-Smgc*). (**B**) Sublingual gland *t-Smgc* transcripts are associated with poly(A^+) RNA. Double-selected poly(A^+) and poly(A^-) RNA fractions and total RNA were added to reverse transcription reactions in the presence (+) and absence (−) of reverse transcriptase, then products were subjected to PCR with primers specific for *Smgc*. PCRs specific for *Muc19* and 18S RNA serve as positive controls for poly(A^+) and poly(A^-) RNA selective transcripts, respectively. Results are representative of two independent experiments. (**C**) Transcripts for *t-Smgc* are not selectively localized to nuclei. Sublingual glands were fractionated into nuclei-containing and nuclei-free fractions. Random primed cDNA prepared from each fraction was PCR amplified with primers specific for *t-Smgc*. Results of three independent preparations are shown. (**D**) Transcripts for *t-Smgc* (823 bp product, upper panel) and *Muc19* are readily detectable by PCR (35 cycles) in random primed cDNA (10 ng) from adult sublingual glands (SLG) but not in submandibular (SMG) or parotid glands. Left side of *t-Smgc* panel, mobilities of 1 kb ladder. Bottom panel, β-actin controls. See Materials and Methods for details.

of Muc19 during mucous cell differentiation. SMGC is highly expressed within terminal bulbs as early as E17, but then progressively decreases within the larger, more-proximal cells of terminal bulbs that undergo transition to acinar cells with the mucous cell phenotype, as manifested by the gradual expansion of apical cytoplasm, basal compression of nuclei, and abundance of cytoplasmic anti-mucin immunoreactivity. Our results are consistent with observations in rats, in which the larger cells of terminal bulbs contain electron-lucent apical granules reactive with anti-mucin antisera (Wolff et al. 2002). Anti-mucin staining then increases progressively during prenatal development as cells accumulate more electron-lucent granules of increasing size (Wolff et al. 2002).

The direct transition of SMGC-expressing cells to cells producing Muc19 is in sharp contrast to acinar cell cytodifferentiation in submandibular glands. SMGC-expressing cells in these glands represent either a completely different cell lineage or an early stage in acinar cell cytodifferentiation that transitions to an intermediate stage (i.e., proacinar exocrine cells) prior to the onset of expression of secretory products of differentiated acinar cells (Denny et al. 1997). Arguing for a role for SMGC in submandibular acinar cell cytodifferentiation is its detection in newly differentiated seromucous acinar cells of rodent submandibular glands (Moreira et al. 1990). We therefore speculate that the initial expression and exocrine packaging of SMGC during development may prime the terminal differentiation of salivary mucous and seromucous acinar cells, perhaps in a manner similar to chromogranin A in neuroendocrine cells. Chromogranin A expression promotes the biogenesis of dense-cored secretory granules and regulates exocrine secretion in neuroendocrine cells (Kim et al. 2001).

During postnatal development, glandular SMGC expression follows a biphasic pattern. First, there is an increase in normalized *Smgc* message levels at E19 and E20. This increase probably results from expansion of the epithelial cell population at the expense of mesenchymal cells, analogous to submandibular glands (Denny et al. 1989). At birth, there is a sudden drop-off in *Smgc* transcript levels, followed by decreased protein levels within 1 to 2 weeks. A possible explanation for this decrease in expression is a stress-related response

caused by an interruption in the glandular supply of nutrients until feeding is initiated (Kuma et al. 2004). The subsequent postnatal increase in *Smgc* transcripts and protein levels coincides with both the rapid expansion of gland mass and the presence of a small subpopulation of SMGC-positive cells, which may represent newly formed acinar cells as part of gland expansion. In addition, we find only minor gender differences in expression of *Smgc* transcripts during postnatal development. In adults of both sexes, transcripts and proteins are barely detectable, with SMGC immunolocalized to intercalated ducts, a potential cellular source for acinar cell regeneration (Denny et al. 1997).

With respect to the small splice variant, *t-Smgc*, we demonstrate that these transcripts are expressed at very low levels in adult sublingual glands, are polyadenylated, and are not sequestered within the nucleus, although putative translated proteins are undetectable. Moreover, the absence of both *t-Smgc* and *Muc19* transcripts in adult submandibular and parotid glands suggests that *t-Smgc* is not a product of non-mucous cell types in salivary glands and may instead be related to Muc19 expression. We hypothesize that *t-Smgc* transcripts represent "slippage" of the splicing machinery during production of *Muc19* transcripts, in which the net interaction between splicing enhancers and silencers allows inclusion of exons 17 and 18 with the subsequent termination of transcription. Alternatively, *t-Smgc* transcripts may represent a regulatory RNA. These RNA species are becoming increasingly identified and can display one or more variable characteristics, including an open reading frame and polyadenylation (Prasanth and Spector 2007).

We find cells expressing SMGC in developing extralobular excretory ducts. In line with a putative role for SMGC in the differentiation of mucin-producing acinar cells, these ductal cells may represent precursors to mucous cells found within mature excretory ducts (Pinkstaff 1980). Alternatively, salivary ductal cells have been shown to take up secreted acinar proteins via endocytosis (Hand et al. 1987; Testa-Riva et al. 1995).

In addition to a switch in the splicing of *Muc19/Smgc* transcripts to initiate expression of Muc19 and the mucous cell phenotype, examination of our collective results provides evidence of additional changes in gene regulation during development that are associated with Muc19 expression. Given that the primary function of mucous cells is to synthesize, package, and secrete Muc19, such changes that can influence the production of Muc19 may thus be considered as transitional stages in mucous cell cytodifferentiation and maturation. We have compiled these changes in gene expression into a working model of key regulatory events during mucous cell development. As shown in Figure 8, initial cytodifferentiation of cells of the terminal bulbs is associated with the initiation of *Muc19/Smgc* transcription and splicing for the production of SMGC and conversion of cells to an exocrine phenotype. The next stage involves mucous cell differentiation, as defined by the production of Muc19. Differentiation is not dependent upon a change in the transcriptional regulation of *Muc19/Smgc*, but instead must involve a switch in the regulation of splicing to produce *Muc19* transcripts rather than *Smgc* transcripts. A simple switch in gene splicing to direct transition from SMGC to Muc19 expression during embryonic development may thus contribute to the early morphological maturation of sublingual glands compared with parotid and submandibular glands (Redman 1988).

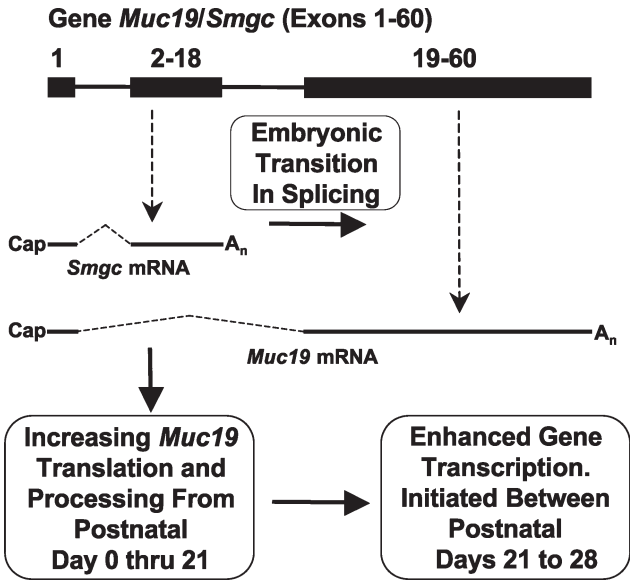

Figure 8 Working model of key mechanisms controlling differential *Muc19/Smgc* gene expression in salivary mucous cells during cytodifferentiation and maturation. A simplified diagram of the gene (top) indicates exon 1 (shared by *Smgc* and *Muc19* transcripts) and two boxes representing exons exclusively utilized either for *Smgc* (2–18) or for *Muc19* (19–60) transcripts. Not drawn to scale. See text for details.

During the first 3 weeks of postnatal development, mucous cells undergo an initial stage of maturation, associated with a progressive and coordinated increase in capacity to translate and process mucin glycoproteins. This maturation stage is evident from the following observations: (1) Normalized levels of *Muc19* mRNA and heteronuclear RNA increase very little during this period, although gland mass increases dramatically, suggesting a relatively stable rate of transcription and splicing of *Muc19* heteronuclear RNA; and (2), normalized levels of mucin glycoproteins, in contrast, increase ~7-fold. The mobilities of mucins during SDS-PAGE are unchanged with age, suggesting that our measurements of mucin levels were not influenced by an increase in the extent of mucin glycosylation. Furthermore, our glycoprotein staining protocol does not differentiate

different patterns of glycosylation; it recognizes both neutral and acidic carbohydrate residues of oligosaccharides (Jay et al. 1990).

Maturation then progresses to a second stage between 21 to 28 days of age, during which the rate of *Muc19/Smgc* transcription is upregulated, producing a 3-fold increase in steady-state levels of *Muc19* mRNA. Because mucous cells comprise more than two-thirds of the gland volume at 3 weeks of age, it is unlikely that the increase in *Muc19* transcripts is due solely to a corresponding increase in the glandular proportion of mucous cells (Hassunuma and Taga 1996). In contrast, during this same period, we find only a slight increase in the level of glandular mucin glycoproteins. We speculate that additional mucins are indeed produced by glands in response to transcriptional upregulation, but are subsequently secreted, so that the total glandular pool of mucins remains relatively stable. A putative increase in mucin secretion during this period may be in response to weaning and the conversion to a solid diet, similar to parotid glands, in which weaning is associated with increased expression of exocrine products, through mechanisms unknown (Redman 1988).

Our model of mucous cell cytodifferentiation and maturation can serve as a framework for the design of future investigations of specific mechanisms that control *Muc19/Smgc* gene expression. For example, targeted deletion of *Smgc* expression, in vivo, may ascertain whether SMGC is required for the terminal differentiation of salivary mucous cells in sublingual tubuloacini as well as in excretory ducts. Comparison of changes in *Muc19* transcripts after weaning pups to a liquid or solid diet would test whether secretion in response to neural reflex pathways associated with taste and mastication are linked to increased transcript levels. Delineation of mechanisms that regulate mucous cell cytodifferentiation may ultimately be incorporated into regenerative or tissue-engineering therapies to treat patients with hyposalivation in response to radiation therapy or autoimmune disease (Kagami et al. 2008).

Acknowledgments

This study was supported by the National Institutes of Health through a RO1 grant (DE014730) to D.J.C. and by funds from a U24 award (DE016509) to R.A. Burne.

The authors thank Bently Robinson, Barbara I. Llanes, Sara Shah, Brandon Schafer, and Maya Yankova for excellent technical assistance.

Literature Cited

Ball WD, Hand AR, Johnson AO (1988a) Secretory proteins as markers for cellular phenotypes in rat salivary glands. Dev Biol 125:265–279

Ball WD, Hand AR, Moreira JE, Johnson AO (1988b) A secretory protein restricted to type I cells in neonatal rat submandibular glands. Dev Biol 129:464–475

Ball WD, Redman RS (1984) Two independently regulated secretory systems within the acini of the submandibular gland of the perinatal rat. Eur J Cell Biol 33:112–122

Chen Y, Zhao YH, Kalaslavadi TB, Hamati E, Nehrke K, Le AD, Ann DK, et al. (2004) Genome-wide search and identification of a novel gel-forming mucin MUC19/Muc19 in glandular tissues. Am J Respir Cell Mol Biol 30:155–165

Culp DJ, Latchney LR, Fallon M, Denny PA, Couwenhoven PC, Sally RI, Chuang S (2004) The gene encoding mouse *Muc19*: cDNA, genomic organization and relationship to *Smgc*. Physiol Genomics 19:303–318

Davies JR, Kirkham S, Svitacheva N, Thornton DJ, Carlstedt I (2007) MUC16 is produced in tracheal surface epithelium and submucosal glands and is present in secretions from normal human airway and cultured bronchial epithelial cells. Int J Biochem Cell Biol 39:1943–1954

Denny PA, Pimprapaiporn W, Bove BJ, Chai Y, Kim MS, Denny PC (1989) Appearance of acinar-cell-specific mucin in prenatal mouse submandibular glands. Differentiation 40:93–98

Denny PC, Ball WD, Redman RS (1997) Salivary glands: a paradigm for diversity of gland development. Crit Rev Oral Biol Med 8:51–75

Escande F, Lemaitre L, Moniaux N, Batra SK, Aubert JP, Buisine MP (2002) Genomic organization of MUC4 mucin gene. Towards the characterization of splice variants. Eur J Biochem 269:3637–3644

Escande F, Porchet N, Bernigaud A, Petitprez D, Aubert JP, Buisine MP (2004) The mouse secreted gel-forming mucin gene cluster. Biochim Biophys Acta 1676:240–250

Fallon MA, Latchney LR, Hand AR, Johar A, Denny PA, Georgel PT, Denny PC, et al. (2003) The sld mutation is specific for sublingual salivary mucous cells and disrupts apomucin gene expression. Physiol Genomics 14:95–106

Hand AR, Coleman R, Mazariegos MR, Lustmann J, Lotti LV (1987) Endocytosis of proteins by salivary gland duct cells. J Dent Res 66:412–419

Hassunuma R, Taga R (1996) Allometric study of the postnatal development of the rat sublingual glands. Okajimas Folia Anat Jpn 73:265–271

Jay GD, Culp DJ, Jahnke MR (1990) Silver staining of extensively glycosylated proteins on sodium dodecyl sulfate-polyacrylamide gels: enhancement by carbohydrate-binding dyes. Anal Biochem 185:324–330

Johnson RF, Mitchell CM, Giles WB, Walters WA, Zakar T (2002) The in vivo control of prostaglandin H synthase-2 messenger ribonucleic acid expression in the human amnion at parturition. J Clin Endocrinol Metab 87:2816–2823

Kagami H, Wang S, Hai B (2008) Restoring the function of salivary glands. Oral Dis 14:15–24

Kim T, Tao-Cheng J, Eiden LE, Loh YP (2001) Chromogranin A, an "on/off" switch controlling dense-core secretory granule biogenesis. Cell 106:499–509

Kuma A, Hatano M, Matsui M, Yamamoto A, Nakaya H, Yoshimori T, Ohsumi Y, et al. (2004) The role of autophagy during the early neonatal starvation period. Nature 432:1032–1036

Laj M, Borghese E, Di Caterino B (1971) Acinar ultrastructure of the sublingual gland of *mus musculus* during embryonic development. J Submicrosc Cytol 3:139–151

Leeson CR, Booth WG (1961) Histological, histochemical, and electron-microscopic observations on the postnatal development of the major sublingual gland of the rat. J Dent Res 40:838–845

Man Y-G, Ball WD, Culp DJ, Hand AR, Moreira JE (1995) Persistence of a perinatal cellular phenotype in submandibular glands of the adult rat. J Histochem Cytochem 43:1203–1215

Moreira JE, Hand AR, Ball WD (1990) Localization of neonatal secretory proteins in different cell types of the rat submandibular gland from embryogenesis to adulthood. Dev Biol 139:370–382

Pinkstaff CA (1980) The cytology of salivary glands. Int Rev Cytol 63:141–261

Prasanth KV, Spector DL (2007) Eukaryotic regulatory RNAs: an answer to the 'genome complexity' conundrum. Genes Dev 21: 11–42

Rasmussen RP (2001) Quantification on the light cycler. In Meuer S, Witter CT, Nakagawara K, eds. Rapid Cycle Real Time PCR, Methods and Applications. Heidelberg, Springer Press, 21–34

Redman RS (1988) Development of the salivary glands. In Sreebny LM, ed. The Salivary System. Boca Raton, CRC Press, 1–20

Redman RS, Ball WD (1978) Cytodifferentiation of secretory cells in the sublingual gland of the prenatal rat: a histological, histochemical and ultrastructural study. Am J Anat 153:367–389

Tabak LA (1995) In defense of the oral cavity: structure, biosynthesis, and function of salivary mucins. Annu Rev Physiol 57: 547–564

Testa-Riva F, Congiu T, Lantini MS, Puxeddu R, Riva A (1995) The main excretory duct (Stensen's) of the human parotid gland: a transmission and scanning electron microscope study. Arch Histol Cytol 58:435–448

Thornton DJ, Rousseau K, McGuckin MA (2008) Structure and function of the polymeric mucins in airways mucus. Annu Rev Physiol 70:459–486

Wolff MS, Mirels L, Lagner J, Hand AR (2002) Development of the rat sublingual gland: a light and electron microscopic immunocytochemical study. Anat Rec 266:30–42

Zinzen KM, Hand AR, Yankova M, Ball WD, Mirels L (2004) Molecular cloning and characterization of the neonatal rat and mouse submandibular gland protein SMGC. Gene 334:23–33

The Journal of Histochemistry & Cytochemistry